Simplified Methodology for Stiffness Estimation of Double D Shaped Caisson Foundations

Pradeep Kumar Dammala[1,2(✉)], Saleh Jalbi[2], Subhamoy Bhattacharya[1,2], and Murali Krishna Adapa[1,2]

[1] University of Surrey, Guildford GU2 7XH, UK
pradeepkumardammala@gmail.com,
s.bhattacharya@surrey.ac.uk,
[2] Indian Institute of Technology Guwahati, Guwahati 781 039, India
salehjalbi@gmail.com, amurali@iitg.ernet.in

Abstract. Foundation stiffness plays a crucial role in the stability analysis of structures to incorporate the Soil Structure Interaction (SSI) effects. Current design approaches of estimating foundation stiffness include advanced dynamic finite element, distributed spring approach, and lumped spring approach. The aim of this paper is to overview the different methods for computing the foundation stiffness and to check their applicability. This has been done by considering an example: Saraighat Bridge supported on double D shaped caisson foundation. Advanced three dimensional finite element analysis is performed to extract the stiffness (Lateral, rotational, and coupling) of double D foundations and the results are compared to the representative circular foundations. It has been concluded that the stiffness of foundation can be significantly affected by its geometry. Furthermore, the stiffness functions are utilized in computing the fundamental frequency of the bridge and also compared with the frequency obtained from different approaches. The frequency estimated using the present study matches satisfactorily well with the monitored data testifying the validation of the work.

1 Introduction

Design engineers require the foundation stiffness for the stability analysis of structures to incorporate the Soil-Structure-Interaction (SSI) effects. The current available approaches in estimating the foundation stiffness include advanced finite/boundary element and Beams on Nonlinear Winkler Foundation (BNWF). Figure 1 schematically illustrates the approaches available for modelling the SSI in case of deep foundations. The BNWF approach (Fig. 1b) lacks the continuity of the soil while the earlier requires highly skilled expertise and is uneconomical. The lumped spring approach proposed by Poulus (1971)—refer to Fig. 1c, represents a simple method to idealize the foundation and surrounding soil using four different types of springs. This approach has been extensively used in dynamic analysis of structures such as offshore wind turbines (Arany et al. 2016; Shadlou and Bhattacharya 2016) and buildings (Gazetas 1991) in predicting the fundamental frequency. It requires the minimum input parameters to

S. Wang et al. (eds.), *New Solutions for Challenges in Applications of New Materials and Geotechnical Issues*, Sustainable Civil Infrastructures,
https://doi.org/10.1007/978-3-319-95744-9_5

estimate the stiffness values for the analysis helping the designer to arrive at a preliminary or approximate geometry of the foundation in a short period of time. In the lumped spring approach, non-dimensional solutions for the stiffness estimation of surface and deep foundations in various directions (vertical-K_V, lateral-K_L, rocking K_R and coupled lateral and rocking-K_{LR}) were proposed by many researchers (Poulus 1971; Banerjee and Davies 1978; Gazetas 1991; Carter and Kulhawy 1992; Higgins and Basu 2011; Shadlou and Bhattacharya 2016; Jalbi et al. 2017).

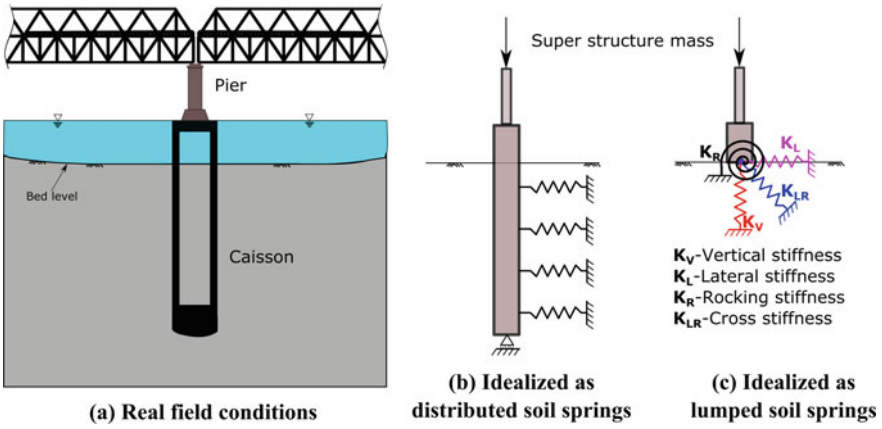

Fig. 1. Idealization of the foundation-soil interaction

Most of the studies are based on either a cylindrical or a rectangular/square shafts embedded in homogeneous/non homogeneous soil column. However, foundations with untraditional geometry may often be required to suit the purpose, such as bridge piers supporting multilane traffic decks in highly scouring rivers. In those cases, caissons of double D or hybrid combination of circular and rectangular sections are preferred, see for example Saraighat Bridge foundation (Dammala et al. 2017a). It is of interest to point out whether the established non-dimensional forms are sufficient enough to analyze an untraditionally shaped foundation or in a nutshell, do the available stiffness formulations take care of geometrical effects of the foundation?

1.1 Objectives

This article highlights the significance of considering geometry effects of rigid caisson foundations on the SSI modelling. A major bridge supported on rigid double D caissons located in a highly active seismic zone is chosen to bring out the importance of including the geometry effects in case of deep foundations. The obtained results in terms of stiffness values are used to estimate the fundamental frequency of the bridge. The same is compared with the frequencies obtained using other available approaches. Furthermore, a final check of fundamental frequency of the bridge pier system is performed with 3D finite element analysis on PLAXIS 3D.

2 Extraction of Lumped Spring Parameters from 3d Fea

A method has been described by Jalbi et al. (2017) to compute the three stiffness terms (K_L, K_{LR}, and K_R) from advanced three dimensional Finite Element Analysis (FEA). A schematic view of the loading conditions along with the idealization is shown in Fig. 2. The vertical stiffness (K_V) is not expected to play a significant role as the caisson foundations are vertically stable and the influencing wave forms are horizontal shear waves. Hence, the K_V is neglected in this study. The linear range of a load-deformation curves can be used to estimate foundation rotations and deflections based on Eq. 1.

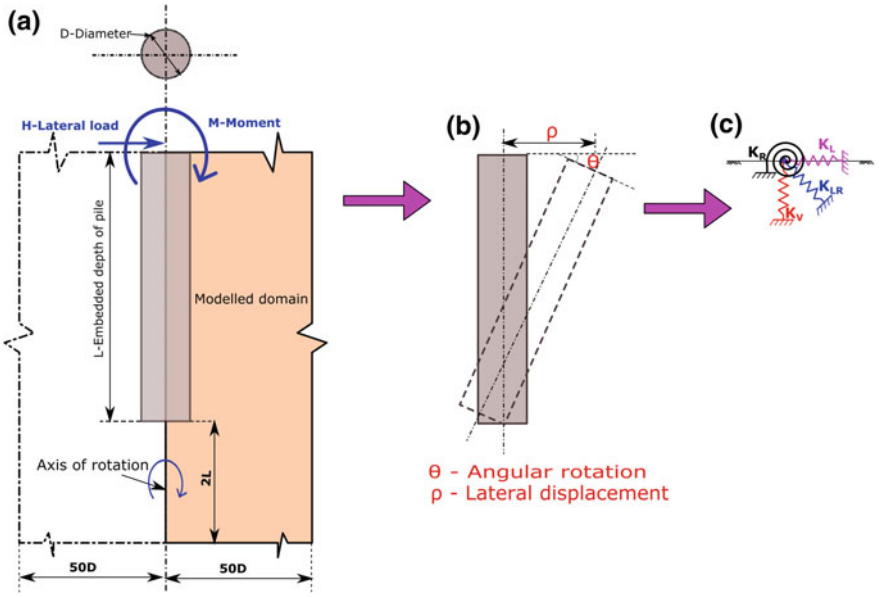

Fig. 2. Schematic representation of **a** soil domain with pile **b** rigid body rotation and translation and **c** idealization as lumped springs

$$\begin{bmatrix} H \\ M \end{bmatrix} = \begin{bmatrix} K_L & K_{LR} \\ K_{LR} & K_R \end{bmatrix} \begin{bmatrix} \rho \\ \theta \end{bmatrix} \tag{1}$$

Equation 1 can be re-written as Eq. 2 where I (Flexibility Matrix) is a 2 × 2 matrix given by Eq. 3

$$\begin{bmatrix} \rho \\ \theta \end{bmatrix} = [I] \times \begin{bmatrix} H \\ M \end{bmatrix} \tag{2}$$

$$I = \begin{bmatrix} I_L & I_{LR} \\ I_{RL} & I_R \end{bmatrix} \tag{3}$$

To obtain the equation unknowns, one can run a numerical model for a lateral load (say H = H_1) with zero moment (M = 0) and obtain values of deflection and rotation (ρ_1 and θ_1). The results can be expressed through Eqs. 4–5.

$$\begin{bmatrix} \rho_1 \\ \theta_1 \end{bmatrix} = \begin{bmatrix} I_L & I_{LR} \\ I_{RL} & I_R \end{bmatrix} \times \begin{bmatrix} H_1 \\ 0 \end{bmatrix} \tag{4}$$

$$\rho_1 = H_1 \times I_L \Rightarrow I_L = \frac{\rho_1}{H_1} \tag{5}$$

$$\theta_1 = H_1 \times I_{RL} \Rightarrow I_{RL} = \frac{\theta_1}{H_1} \tag{6}$$

Similarly, another numerical analysis can be done for a defined moment (M = M_1) and zero lateral load (H = 0) and the results are shown in Eqs. 7–8.

$$\begin{bmatrix} \rho_2 \\ \theta_2 \end{bmatrix} = \begin{bmatrix} I_L & I_{LR} \\ I_{RL} & I_R \end{bmatrix} \times \begin{bmatrix} 0 \\ M_1 \end{bmatrix} \tag{7}$$

$$\begin{aligned} \rho_2 &= M_1 \times I_{LR} \Rightarrow I_{LR} = \frac{\rho_2}{M_1} \\ \theta_2 &= M_1 \times I_R \Rightarrow I_R = \frac{\theta_2}{M_1} \end{aligned} \tag{8}$$

From the above analysis (Eqs. 4–8), terms for the I matrix (Eq. 3) can be obtained. Equation 2 can be rewritten as Eq. 8 through matrix operation.

$$[I]^{-1} \times \begin{bmatrix} \rho \\ \theta \end{bmatrix} = \begin{bmatrix} H \\ M \end{bmatrix} \tag{9}$$

Comparing Eqs. (1 and 9), the relation between the stiffness matrix and the inverse of flexibility matrix (I) given by Eq. 10. Equation 11 is a matrix operation which can be carried out easily to obtain K_L, K_R and K_{LR}.

$$K = \begin{bmatrix} K_L & K_{LR} \\ K_{RL} & K_R \end{bmatrix} = I^{-1} = \begin{bmatrix} I_L & I_{LR} \\ I_{RL} & I_R \end{bmatrix}^{-1} \tag{10}$$

$$K = I^{-1} = \begin{bmatrix} \frac{\rho_1}{H_1} & \frac{\rho_2}{M_2} \\ \frac{\theta_1}{H_1} & \frac{\theta_2}{M_2} \end{bmatrix}^{-1} \tag{11}$$

Therefore, mathematically, two FEA analyses are required to obtain the three spring stiffness terms. It is important to note that the above methodology is only applicable in the linear range and it is advisable only to use the obtained stiffness values for Eigen frequency analysis or a first estimate of the deformations using Eq. 1.

3 Numerical Model

Finite element analysis package PLAXIS 3D has been used in this study where the soil is idealized as an isotropic linear elastic material. A "Rigid Body" option has been set to the foundation where it is restricted to deform axially or in bending, and only the surrounding soil is mobilized. This assumption is valid since the well foundation has a low aspect ratio (due to the high diameter/width) and also because concrete has higher flexural and shear stiffness than soil. The interface between the soil and foundation had the same stiffness properties as the surrounding soil and a very fine mesh was implemented for enhanced accuracy.

The extent of the soil contour was taken as at least 50D (D is the diameter) and the depth h (h is the depth of the soil stratum) was at least twice that of the foundation. The objective was to ensure the stresses in the soil are not affected by the vicinity of the translational boundary conditions at the sides and bottom face (Figs. 2 and 3). Previous work presented in Krishnaveni et al. (2016) modelled the stratum with 5D width, whilst

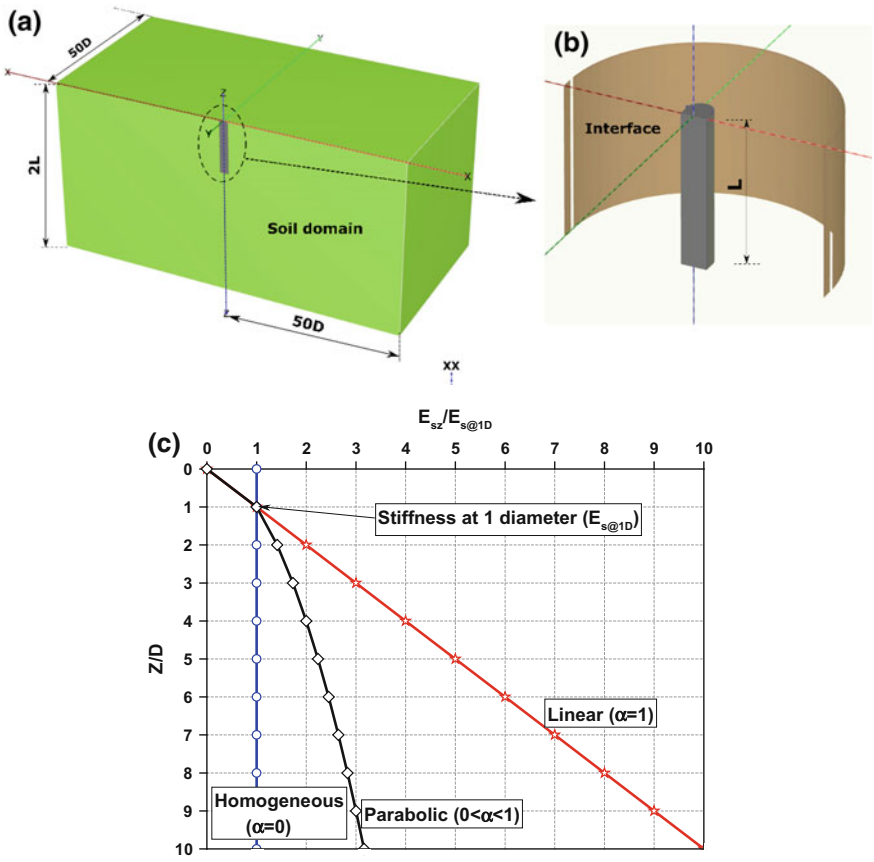

Fig. 3. **a** Numerical model geometry **b** Double D with the rigid SSI **c** Stiffness variation with depth

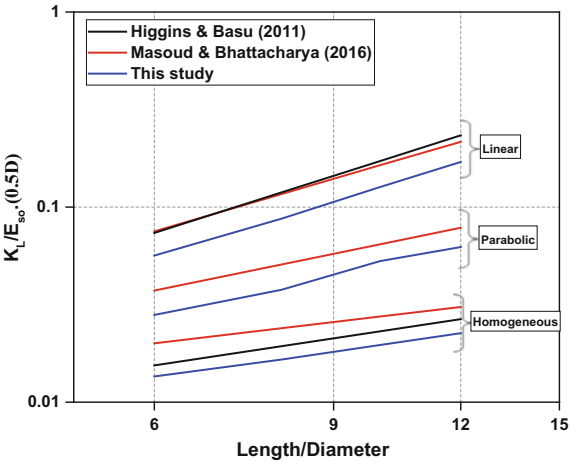

Fig. 4. Variation of normalized lateral stiffness

Abbas et al. (2008) used 40D on finite element software to analyze laterally loaded piles, which shows a wide range of selected soil extents. To save computational power and operational time cost, only half the system was modelled due to symmetry.

PLAXIS 3D also allows the user to define either a constant stiffness or stiffness increasing linearly with depth. These two settings were applied to idealize homogenous and linear ground profiles, respectively. For parabolic variation of soil stiffness, the soil stratum was discretized with multiple layers where each layer with a thickness of 0.025 h. An initial stiffness value and linear slope was input to each layer to represent a parabolic stiffness variation. Homogeneous soils are soils which have a constant stiffness with depth such as over-consolidated clays. On the other hand, a linear profile is typical for normally consolidated clays [or "Gibson Soil" (Gibson 1974)] and parabolic behaviour can be used for sandy soils, see Fig. 3c.

The software also has the capability to model the initial stresses in the stratum and the change in the stress state due to the construction sequence. Accordingly, the displacements were set to zero prior to application of the loads and values for K_L, K_R, and K_{LR} were computed. The first phase of loading consists of a lateral load of 100 kN (X-axis) with no moments acting while the second phase consists of 100 kN moment in the secondary axis (Y-axis) with no lateral loads. The displacements (both lateral and axial) are monitored during the loading and the stiffness values are evaluated as explained earlier.

3.1 Model Validation

In order to check the efficiency of the numerical modelling and the extracted results, the developed model is validated with the published literature (Higgins and Basu 2011; Shadlou and Bhattacharya 2016) of rigid circular foundations as there are no solutions for double D foundations. Higgins and Basu (2011) proposed non-dimensional formulations to estimate the stiffness of rigid piles in soils of uniform stiffness

(homogeneous) and linearly varying stiffness. Similarly, Shadlou and Bhattacharya (2016) proposed such stiffness formulations for both rigid and flexible piles for a wide range of L/D ratio, where L represents the embedded depth and D is the diameter of the pile.

To validate the developed model results for double D, a circular shaft of diameter 5 m is chosen with varying length (30–60 m) representing L/D ratio of 6–12. The soil column is modelled using the three profiles, homogeneous, linear and parabolic stiffness variation. The elastic modulus of the soil is chosen as 100 MPa for the homogeneous profile while for linearly varying stiffness, the incremental stiffness is calculated based on the diameter of the shaft. However, for the parabolic stiffness, soil is discretized into many layers and then the corresponding initial stiffness and the incremental stiffness for each layer are defined accordingly. The loading is applied as discussed earlier.

Once the lateral and axial displacements at the caisson head are monitored for each loading, then the rotation is calculated using which the stiffness values are estimated. The stiffness functions are normalized using the soil stiffness (E_{so}) and the radius of the section (r). Figure 4 presents the variation of normalized length (L/D) with the normalized lateral stiffness for different soil profiles along with the comparative literature. It can be inferred from the Fig. 4 that the present model shows a consistent trend with increase in L/D ratio in spite of the nominal difference in the magnitude. This difference is mainly attributed due to the numerical modelling and can be ignored as the magnitude of difference is ±5%. Similarly, normalized K_R and K_{LR} are also presented in Figs. 5 and 6. Hence, the method of extraction is appropriate and can be used to estimate the stiffness of double D shaped foundations.

Once the stiffness of the foundation is established, the results can be used for the quick dynamic analysis of the structures supported on such foundations. Such dynamic analysis was performed by Arany et al. (2016) and Shadlou and Bhattacharya (2016) to identify the fundamental frequency of offshore wind turbines on using the lumped soil springs.

3.2 Saraighat Bridge

A bridge (Saraighat Bridge) supported on Double D caisson foundation is chosen to illustrate the significance of considering the geometry in the analysis. Saraighat Bridge is a double decker bridge supporting both roadway and railway over the piers and resting on double D caissons, see Fig. 7. The schematic representation of the bridge with the foundation details is shown in Fig. 8. This bridge is located in a very high seismic active zone in India (Assam). Further details about the bridge can be found in Dammala et al. (2017a).

The double D shaped caisson in this case is represented by two parameters for easy presentation, the diameter D and the width B as shown in Fig. 8c. It is modelled as (Fig. 8d) a rigid body due to the sheer size of the foundation. The embedment depth of the foundation is 41 meters and the surrounding soil is modelled using the homogeneous, linear and parabolic variation of stiffness with the appropriate soil parameters considered from Dammala et al. (2017b). Positive interface elements are considered with the stiffness of interface equals to that of surrounding soil (Fig. 8d). A horizontal

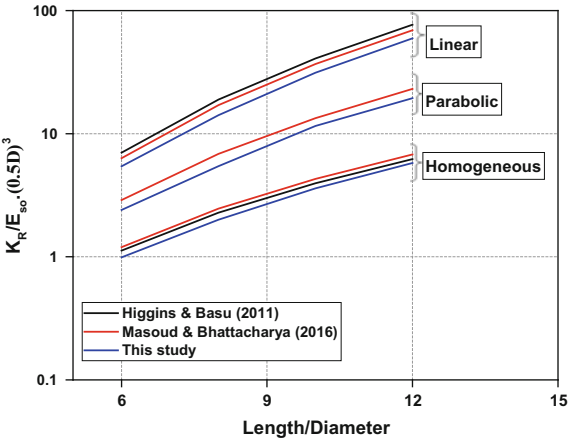

Fig. 5. Variation of normalized rocking stiffness

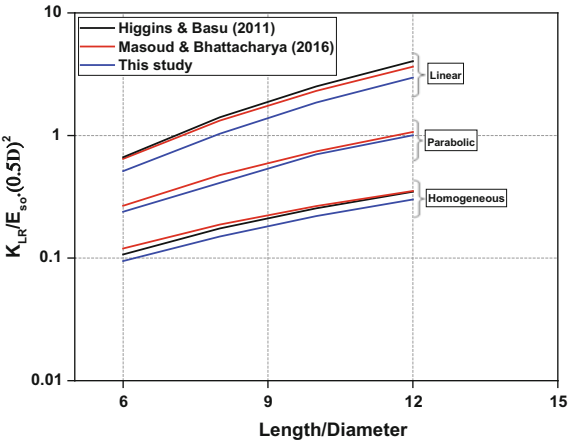

Fig. 6. Variation of normalized coupled rocking and lateral stiffness

load of 100 kN and a moment of 100 kN m is applied at the ground surface (bed level). Firstly, the extracted K_L, K_R, and K_{LR} values obtained directly from the FEA will be compared to the representative circular shaft computed based on solutions provided in the literature.

4 Results

Initially, two types of analysis is performed in homogeneous soil conditions, one with the double D shaped and the other with the circular shaft of representative diameter (9.6 m). Table 1 lists the horizontal (ρ_x) and axial (ρ_z) deformations at shaft head, for

Fig. 7. Saraighat Bridge, Assam, India

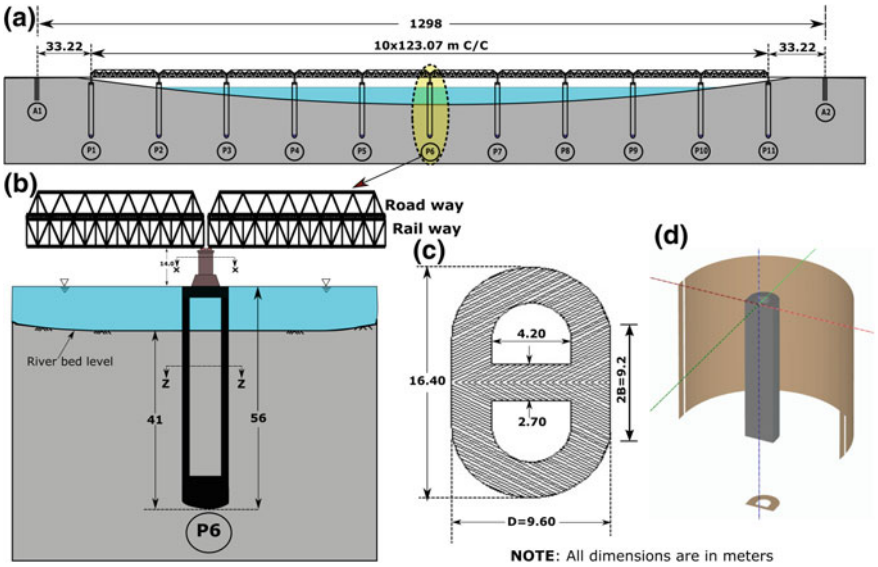

Fig. 8. Schematic view of **a** Saraighat Bridge, **b** central pier, **c** well foundation and **d** developed numerical model with interaction

both the cases in all the soil conditions. It is evident from the results that the displacements experienced by the double D caisson are significantly lower than that of representative circular shaft testifying the efficiency of double D over circular shafts.

Table 1. Displacements in lateral and axial directions in both the cases for homogeneous soil condition

Displacement direction	Circular section		Real geometry		% Difference	
	H = 100, M = 0	H = 0, M = 100	H = 100, M = 0	H = 0, M = 100	H = 100, M = 0	H = 0, M = 100
Lateral	0.08	0.002	0.05	0.007	60	185
Axial	0.01	0.004	0.001	0.0002	900	1900

The stiffness values obtained from the analyses for the double D are compared with the stiffness estimated for the circular shaft based on Shadlou and Bhattacharya (2016) rigid shaft formulations. Table 2a–c present the results in terms of stiffness values (K_L, K_R and K_{LR}) for both the geometrical conditions, at each soil profile. It is quite interesting to note that the stiffness of double D caisson is remarkably higher than that of circular shafts. An increase of almost 30–50% is noted in all the cases. This increase in impedance is obviously attributed due to the higher resistance offered by the rectangular portion of the double D caisson.

Table 2. Comparison of lateral stiffness obtained from circular assumption and real geometry

a			
Profile	Lateral stiffness (K_L)		
	Circular (Shadlou and Bhattacharya 2016)	Real geometry (PLAXIS)	%Δ
Homogeneous	7.66	9.77	27
Linear	20.63	29.24	41
Parabolic	12.13	17.07	40
b			
Profile	Rotational stiffness (K_R)		
	Circular (Shadlou and Bhattacharya 2016)	Real geometry (PLAXIS)	%Δ
Homogeneous	5328	7594	42
Linear	19890	30358	52
Parabolic	10712	15156	41
c			
Profile	Coupled stiffness (K_{LR})		
	Circular (Shadlou and Bhattacharya 2016)	Real geometry (PLAXIS)	%Δ
Homogeneous	156	204	30
Linear	597	869	45
Parabolic	296	419	41

5 Natural Frequency Computation—Application

The simulated values of K_L, K_R and K_{LR} of the double D caisson are utilized in estimating the fundamental frequency (f_{nz}) of the bridge piers. As the underlying soil near the bridge is predominantly sandy soil with varying density along the depth (Dammala et al. 2017b), a linear variation of stiffness assumption would suit better, and hence adopted the stiffness functions of linear stiffness variation from the present study. A simple stick model (Fig. 1c) with a lumped mass at the pier head is considered to model the bridge pier system with the properties presented in Dammala et al. (2017a). A f_{nz} of 1.05 Hz is obtained by performing linear Eigen vector modal analysis on the soil well pier system. Debnath et al. (2016) estimated the f_{nz} of the Saraighat Bridge pier system to vary between 0.9031–0.9119 Hz based on operational modal analysis. Apart from this, Dammala et al. (2017a) performed similar Eigen vector modal analysis using the distributed spring approach and arrived at an f_{nz} of 0.8547 Hz.

In order to better check the present results, a three dimensional (3D) finite element program (PLAXIS 3D) is employed to model the entire support system of the bridge at the central part (Pier 6). The caisson is embedded in the loose sandy soil from the ground surface to a depth of 11 m followed by a dense deep sand of 30 m thickness, further followed by a clay layer of 30 m deep. Appropriate structure and soil properties along with the loading on the bridge deck are considered from the literature (Dammala et al. 2017a). Figure 9 shows the developed model. A static lateral load is applied at the pier head to perform a free vibration analysis of the structure (Fig. 9b). The load is

taken off in the next phase allowing the structure to vibrate freely (50 s) in order to monitor the free decay of the system. Similar analysis is presented for a building in the tutorial manual of PLAXIS 3D (PLAXIS 2013).

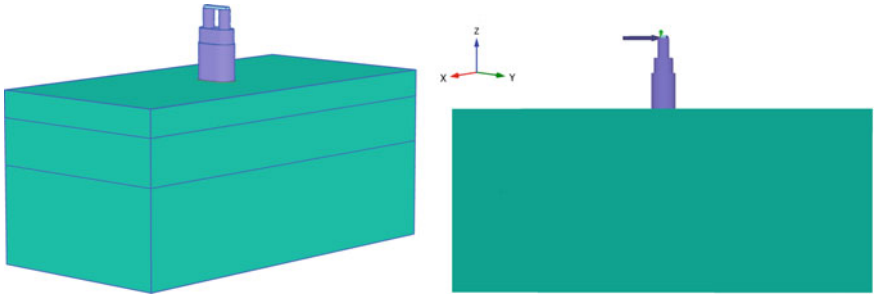

Fig. 9. Numerical model of the entire Soil-Well-Pier system along with the pier head loading

The deformed contours of the soil well pier system is shown in Fig. 10, where almost no significant displacements can be observed in the soil while the pier experienced a maximum displacement of 0.557 mm. The free vibration decay of the system is shown in Fig. 11a, b. The enlarged view of the free decay as shown in Fig. 11b represents a fundamental period of 1.30 s (f_{nz} = 0.769 Hz). Although this is narrowly different to the monitored frequency of the bridge (0.90 Hz), it gives an idea that the range of frequency could possibly fall between 0.70 and 1 Hz. The f_{nz}

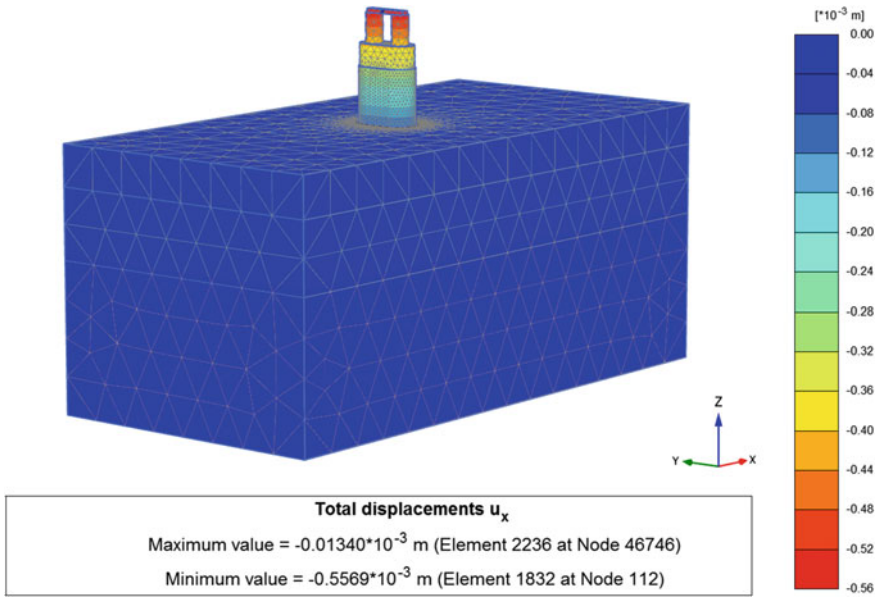

Fig. 10. Deformation contours of the soil well pier system

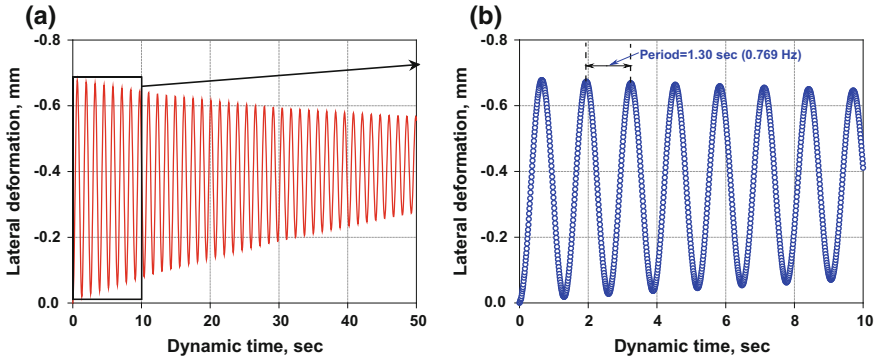

Fig. 11. **a** Free vibration decay of the SWP system, **b** Enlarged view briefing the fundamental period

obtained from the lumped spring approach could satisfactorily catch the response of the system although the stiffness functions utilized are obtained from the static impedance functions without considering the soil stiffness degradation and damping characteristics. It may well be inferred that on inclusion of stiffness degradation, the f_{nz} may further decrease which could possibly yield a closer agreement with the monitored data. Table 3 lists the f_{nz} from various approaches and the percentage difference.

Table 3. Comparison of f_{nz} using different approaches

Approach	Monitored data (Debnath et al. 2016)	Distributed springs (Dammala et al. 2017a)	Lumped springs (This study)	Numerical approach (PLAXIS 3D)
f_{nz} (Hz)	0.903	0.855	1.05	0.769
%Δ with monitored data	–	−5.3	+16.28	−14.84

6 Conclusions

The available stiffness formulations for the analysis of rigid deep foundations are based on either traditional circular shafts or on rectangular or square geometry. This study highlights the significance of having the geometry based non-dimensional formulations for stiffness estimation with a case study. A bridge located in a highly active seismic zone resting on massive double D caisson shaped foundations was chosen for illustration. The stiffness of the caisson in both the cases (circular and double D) is estimated using advanced finite element program. Three soil profiles with homogeneous, linear and parabolic stiffness variation are considered in the analysis. The results indicate that the geometry of the foundation do effect the stiffness, mostly the rotational stiffness due to the resistance offered by the rectangular section. Furthermore, the

developed stiffness values are utilized in determining the fundamental frequency of the bridge pier system and a reasonably close match is achieved with the extracted stiffness values. Further soil stiffness degradation and damping characteristics need to be considered to enhance the efficiency of the highlighted geometry effects. Since the fundamental frequency calculated using the lumped springs provided a reasonable estimate, further scope of the work is required to develop such geometry based stiffness non-dimensional forms for easy-to-use in the design offices for preliminary analysis and design.

Acknowledgements. The first author would like to thank the Commonwealth Scholarship Commission (CSC) for providing him the financial support (reference no: INCN-2016-214) enabling him to perform his research activities in the University of Surrey, United Kingdom. The funding received is fully acknowledged.

References

Abbas, J.M., Chik, Z.H., Taha, M.R.: Single pile simulation and analysis subjected to lateral load. Electron. J. Geotech. Eng. **13** (2008)

Arany, L., et al.: Closed form solution of eigen frequency of monopile supported offshore wind turbines in deeper waters incorporating stiffness of substructure and SSI. J. Soil Dyn. Earthq. Eng., Elsevier, (2016). https://doi.org/10.1016/j.soildyn.2015.12.011

Banerjee, P.K., Davies, T.G.: The behavior of axially and laterally loaded single piles embedded in non-homogeneous soils. Geotechnique (1978). https://doi.org/10.1680/geot.1978.28.3.309

Carter, J.P., Kulhawy, F.H.: Analysis of laterally loaded shafts in rock. J. Geotech. Eng. ASCE (1992). https://doi.org/10.1061/(ASCE)0733-9410(1992)118:6(839)

Dammala, et al.: Scenario based seismic re-qualification of caisson supported major bridges—a case study of Saraighat Bridge. J. Soil Dyn. Earthq. Eng. (2017a). https://doi.org/10.1016/j.soildyn.2017.06.005

Dammala, et al.: Dynamic soil properties for seismic ground response studies in Northeastern India. Soil Dyn. Earthq. Eng. **100**, 357–370 (2017b). https://doi.org/10.1016/j.soildyn.2017.06.003

Debnath, N., et al.: Multi-modal vibration control of truss bridges with tuned mass dampers under general loading. J. Vibr. Control (2016). https://doi.org/10.1177/1077546315571172

Gazetas, G.: Formulas and charts for impedances of surface and embedded foundations. J. Geotech. Eng. ASCE (1991). https://doi.org/10.1061/(ASCE)0733-9410(1991)117:9(1363)

Gibson, R.: The analytical method in soil mechanics. Geotechnique **24**, 115–140 (1974)

Higgins, W., Basu, D.: Fourier finite element analysis of laterally loaded piles in elastic media. International Geotechnical Report, University of Connecticut, US (2011)

Jalbi et. al.: Practical method to estimate foundation stiffness for design of offshore wind turbines. Wind Energy Eng.: A handbook for onshore and offshore wind turbines, 329 (2017)

Krishnaveni, B., Alluri, S.K.R., Murthy, M.R.: Generation of p-y curves for large diameter monopiles through numerical modelling. Int. J. Res. Eng. Technol. (2016)

Plaxis, B.V.: PLAXIS 3D 2013 Reference Manual. PLAXIS BV, Delft (2013)

Poulos, H.: The displacement of laterally loaded piles: I-single piles. J. Soil Mech. Found. Div. **97**, 711–731 (1971)

Shadlou, M., Bhattacharya, S.: Dynamic stiffness of monopoles supporting offshore wind turbine generators. J. Soil Dyn. Earthq. Eng., Elsevier, (2016). https://doi.org/10.1016/j.soildyn.2016.04.002